



# REPORT: GEOSTATISTICAL ANALYSIS OF CO-NI DEPOSIT USING KRIGING

Submitted as a requirement for  
Geomodelling course

by  
Sai pavan kumar Yedduri

## **Table of Contents**

- 1. Geostatistical Analysis of the Copper and Nickel Compositions**
  - 1.1. Exploratory Data Analysis on Co–Ni Deposit Data**
    - 1.1.1. Analysis Based on Properties of the Data
      - a. Identifying Unusual Properties
      - b. Outliers and Anomalies
    - 1.1.2. Histograms (Co and Ni) / Skewness
    - 1.1.3. Outliers Identified from Boxplots
    - 1.1.4. Optical Impressions in Spatial Maps and Bindings
    - 1.1.5. Tectonic Faults or Hops
    - 1.1.6. Correlation / Dependencies
    - 1.1.7. Observations vs. Expectations
    - 1.1.8. Other Problems
  - 1.2. Variogram Analysis on Co–Ni**
    - 1.2.1. Variogram Cloud
    - 1.2.2. Check for Anisotropy
    - 1.2.3. Fit for Variogram Model
  - 1.3. Kriging**
  - 1.4. Cross Validation: Evaluation of Kriging Analysis**
- 2. Kriging Analysis Based on High Concentrations and Low Concentrations**
  - 2.1. Comparison of subregions kriging a with Overall-Area Results

## 1. Exploratory Data Analysis on Co-Ni deposit data:

A statistical data analysis has been performed for the given Cobalt (Co) and Nickel (Ni) concentrations at the location's "x" and "y" as per the data. Data visualization of the Co and Ni would provide more insights into the distribution, relationships, and potential geological anomalies.

### 1.1.1. Analysis based on properties of data:

1. Identifying unusual properties:
  - a. There are some outliers apart from the uniform grid.
  - b. The "Co" concentration is represented as point size, which falsely implied as a fault.
  - c. There are overlays present due to neighborhood of higher concentrations.

### 1.1.2. Histogram (Co and Ni)/Skewness:

From the histograms of Co and Ni, it is evident that both distributions are very close to normal/gaussian distribution, despite slight left-skewness's and long tailed. Q-Q plot also confirms this, showing a positive correlation of the data with respect to theoretical quantiles of normal distribution.

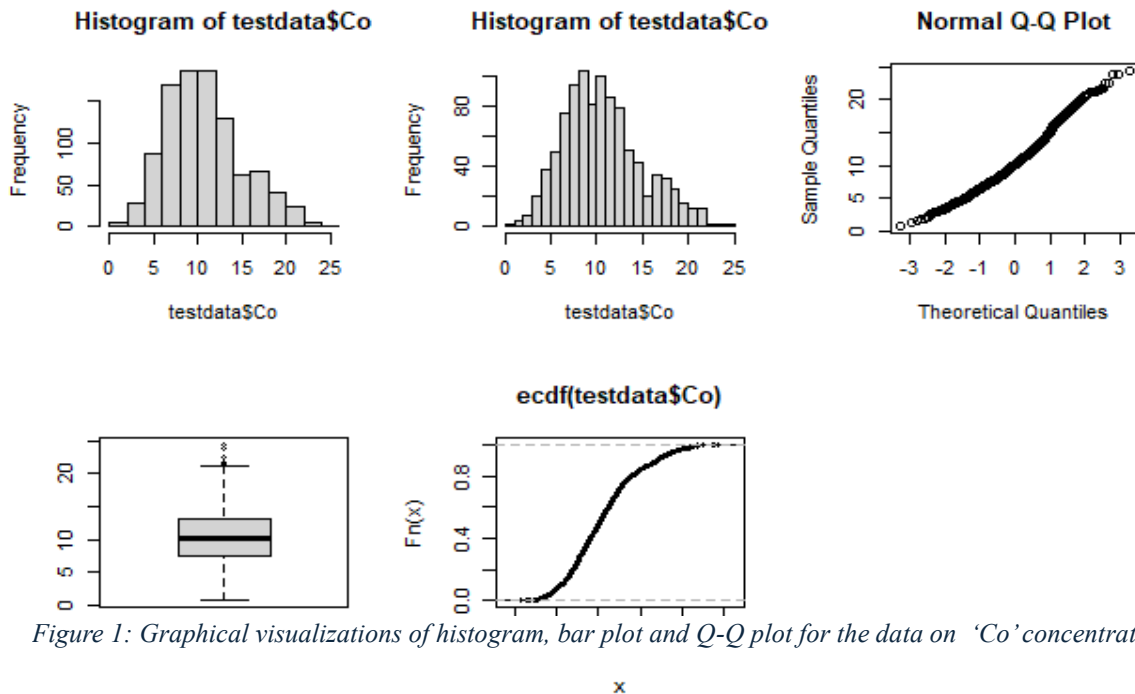


Figure 1: Graphical visualizations of histogram, bar plot and Q-Q plot for the data on 'Co' concentration

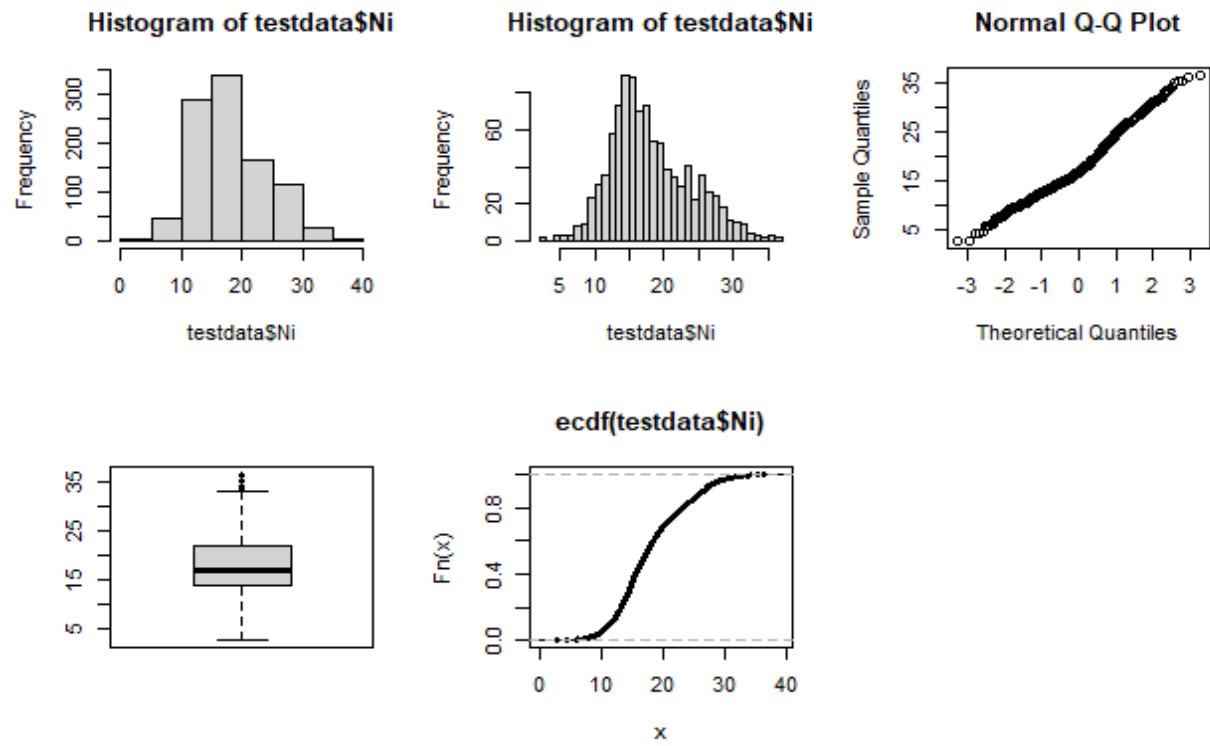


Figure 2: Graphical visualizations of histogram, bar plot and Q-Q plot for the data on 'Ni' concentration.

### 1.1.3. Outliers Identified from Boxplots:

From boxplots of Fig1 and Fig2, both Co and Ni exhibit outliers at higher concentrations. The location of the outliers can be identified in Fig3 represented by a cross symbol.

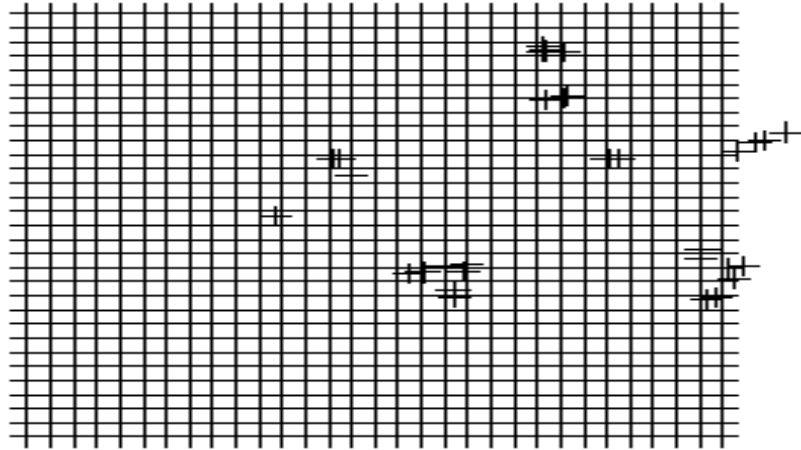
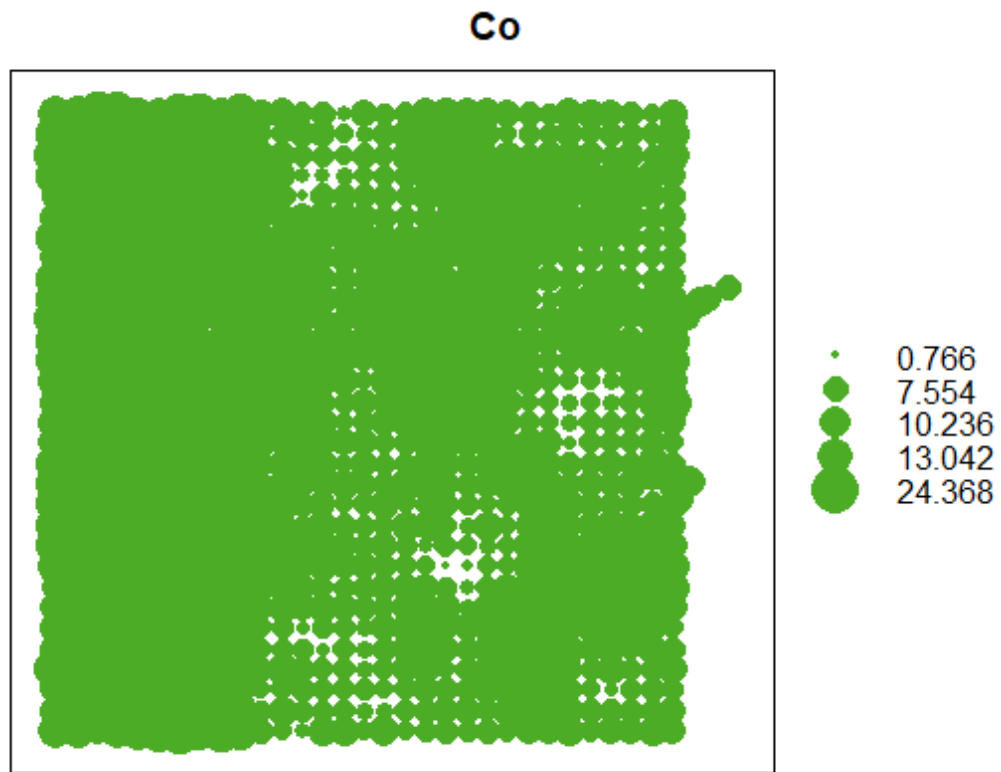


Figure 3: Grid indicating measurement locations  $(x, y)$  for the data points with outliers.

#### 1.1.4. Optical impressions in spatial maps and bindings:

Since, the concentration of Co and Ni were represented with marker size. overlapping of the neighboring high concentrations might imply misinterpretation of actual variation in the data.



*Figure 4: Visualization of 'Co' concentration by marker size*

There is visible evidence of Overlays in both Co and Ni. This could be due to binding/rounding errors while measuring the data.

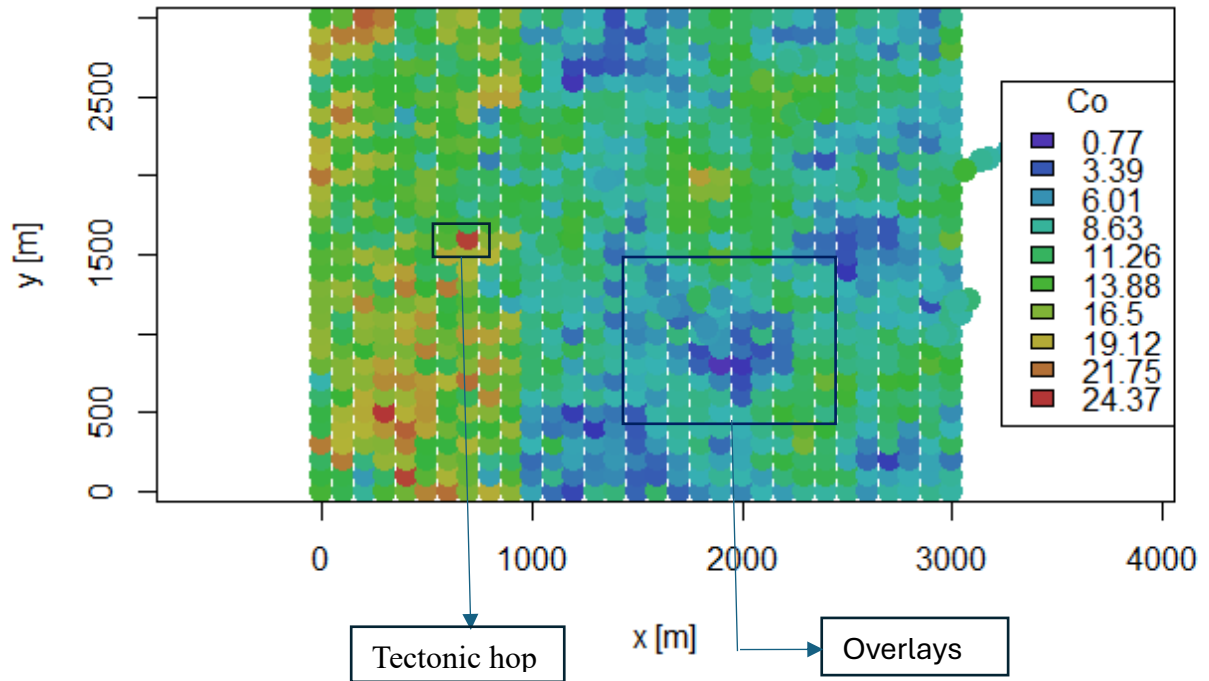


Figure 5: Visualization of 'Co' concentration by color indicating faults due to optical impression.

1.2. In general, most of the high concentrated Co lie on the left side and low concentrated Co lie on the right side.

1.1.5. Tectonic faults or hops: There are observable discontinuities in concentration of both Co and Ni, suggesting tectonic faults.

### 1.1.6. Correlation / Dependencies

1. The concentrations of Co and Ni are moderately positively correlated with linear correlation of 0.519
2. Similarly, horizontal location("x") is moderately negatively correlated with Co and Ni at -0.534 and -0.68 respectively. On the other hand, the Co and Ni concentrations are almost linearly correlated longitudinally.

	X	x	y	Co	Ni
X	1.00000000	0.132573864	0.487331023	-0.04336849	-0.07545011
x	0.13257386	1.000000000	0.008204151	-0.53736541	-0.68002821
y	0.48733102	0.008204151	1.000000000	0.02671672	-0.04970914
Co	-0.04336849	-0.537365407	0.026716722	1.00000000	0.51870446
Ni	-0.07545011	-0.680028214	-0.049709141	0.51870446	1.00000000

Table 1: Table of correlation between locations and concentrations of Co and Ni.

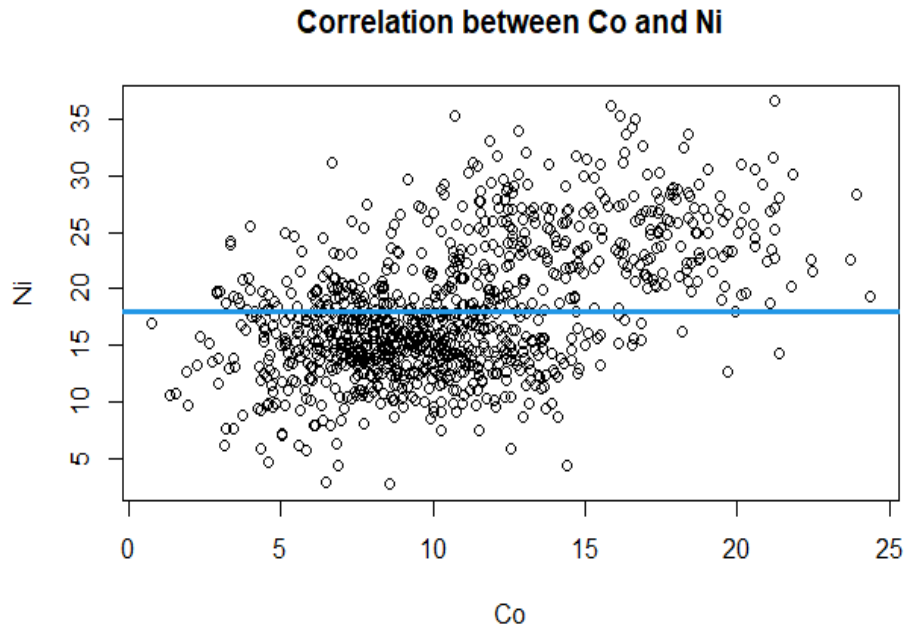


Figure 6: Correlation between concentrations of Co and Ni



#### **1.1.7. Observations vs. Expectations**

The weaker correlation between Co and Ni may suggest differential mobility during geochemical processes.

The outliers apart from the uniform location of data points were not expected. These outliers' concentration might be responsible for deviation of Co, Ni histograms with their ideal gaussian distributions.

#### **1.1.8. Other Problems**

While grid is uniform, there are anomalies at high values. These could be the measuring or rounding errors.

## 1.2 Variogram Analysis on Co-Ni:

### 1.2.1. Variogram cloud

- From the variogram cloud, there are some outliers/extreme values of semi variances at long distances (as it reaches 1500m)
- From visual inspection, pairs are frequently observed below 1000m.

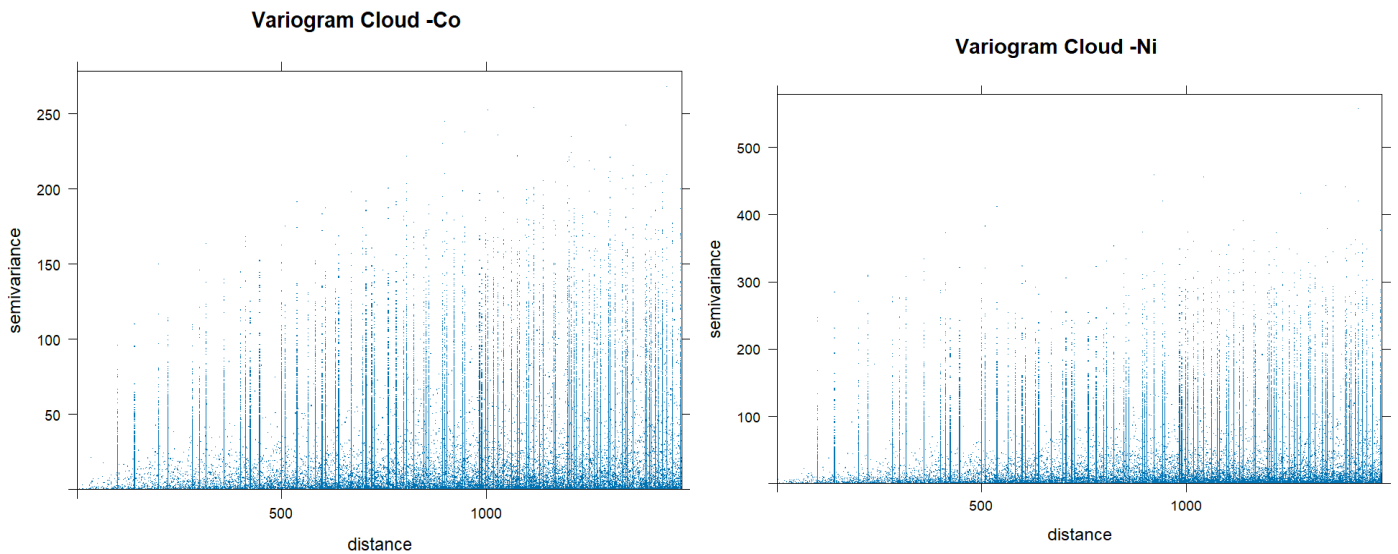


*Figure 7: Variogram clouds for Co and Ni*

### 1.2.2. Check for anisotropy:

a. The Variogram maps of both Co and Ni reveal anisotropy:

The variogram maps of Co and Ni, as shown below, don't follow symmetric distribution of variance concentrations along x and y.

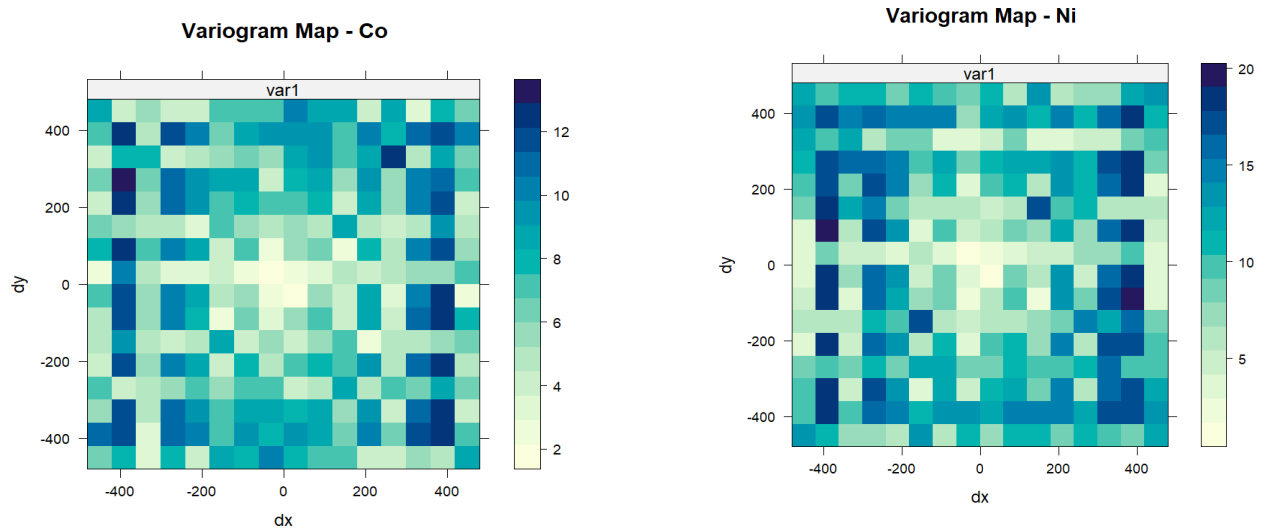


Figure 8: Variogram maps for Co and Ni

### **1.2.3. Fit for Variogram model:**

Initially, a reasonable fit was achieved with an exponential variogram for Co and spherical variogram for Ni, as shown in Figure 10.

The essential parameters for defining an exponential variogram for Co:

2.1.5. Semivariance increases and stabilizes around range of 1250m

2.1.6. The sill is considered approx. 18

2.1.7. Nugget is considered approx. 2.

The essential parameters for defining exponential variogram for Ni:

i. Semi variance increases and stabilizes around range of 1400m

ii. The sill is considered approx. 30

iii. Nugget is considered approx. 2

But, because of the anisotropy of Co and Ni concentrations from the variogram maps above, exponential variogram model for Co and spherical variogram model for Ni doesn't fit the data at 0, 45, 90, 135, 180 degrees.

From figure 9, though a reasonable fit has been observed at 135 degrees for Co and 45 degrees for Ni. The model doesn't fit at other angles. This confirms the presence of anisotropy along different angles.

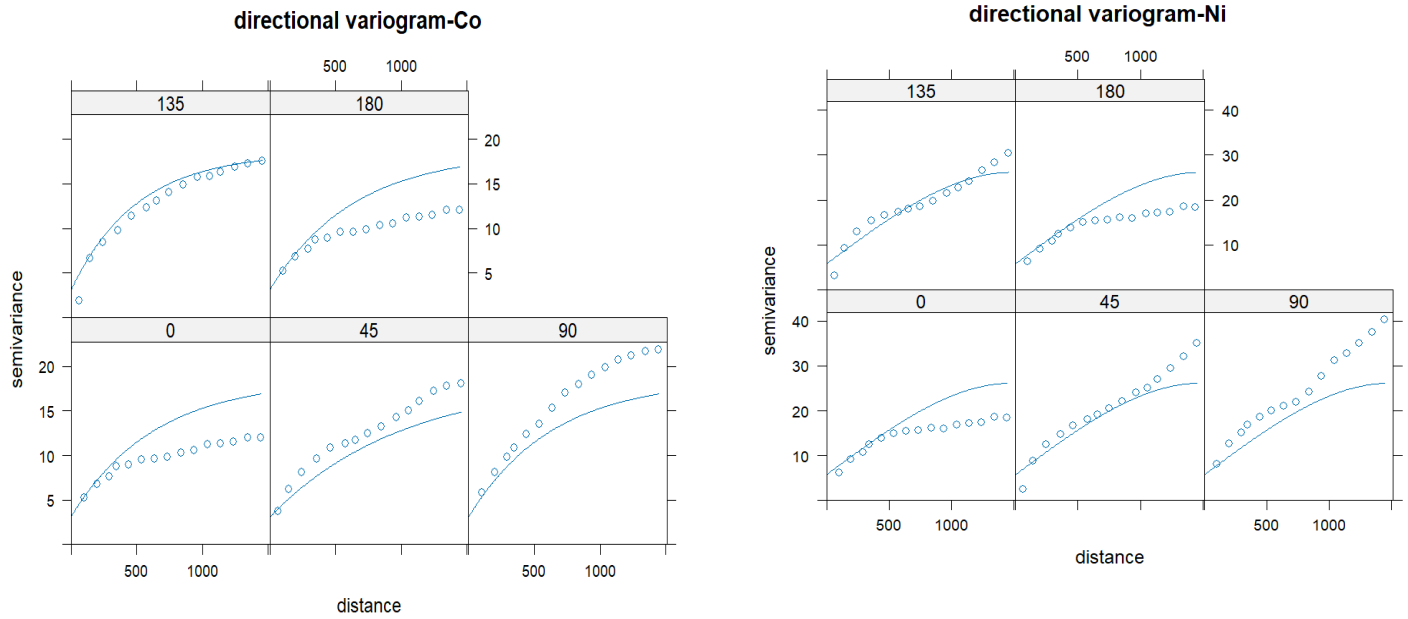


Figure 9: Directional fit of the exponential model for Co and spherical model for Ni at 0,45,90,135 and 180 degrees.

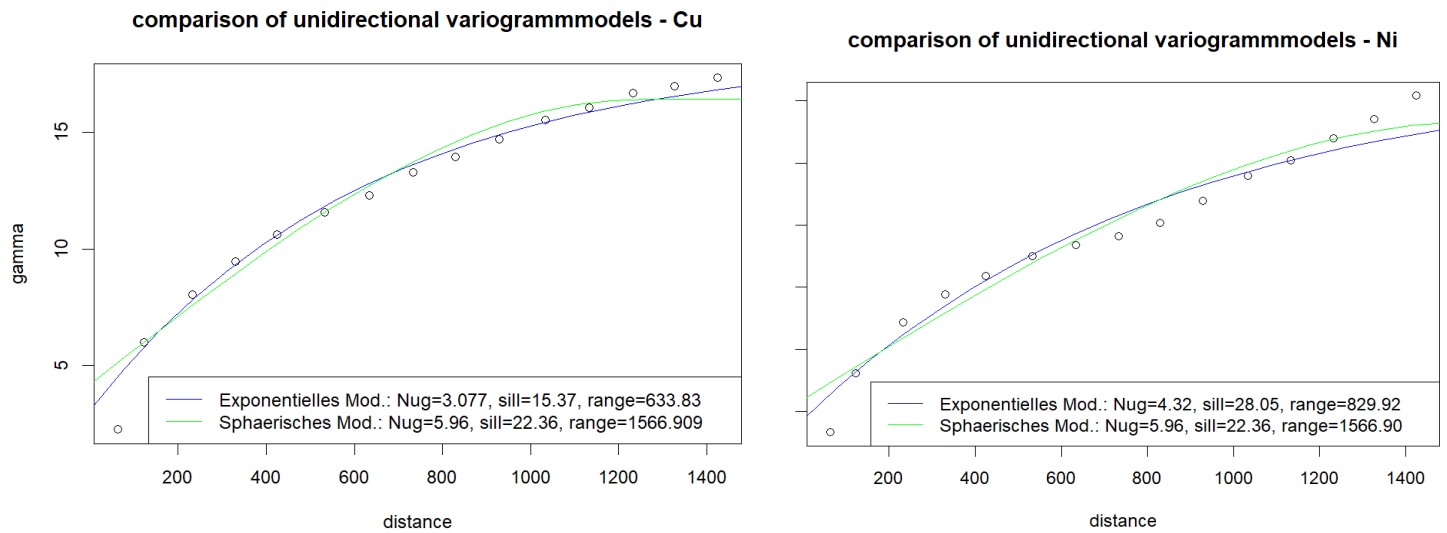


Figure 10: Comparison of exponential and spherical variogram models for Co and Ni, indicating nugget, sill and range.

### 1.3. Kriging

Before applying kriging, a regular grid of points (with 10-unit spacing) is created resulting in spatial grid. The same grid is used for estimation of both Co and Ni concentrations.

The data exploration analysis and check for anisotropic suggested that there is no deterministic trend in the coordinates and no external global is known. Therefore, ordinary kriging is preferred to estimate uncertainty locations across the grid. Ordinary kriging estimates at an unknown point by considering means of neighborhood.

The ‘Co’ and ‘Ni’ concentrations are predicted across the grid with respect to known certainty which are referred to as `var1.pred` and `var1.var` in Figure11 and Figure12 respectively.

`var1.pred`: Kriging estimate of Co or Ni across the grid area.

`var1.var`: Kriging variance —i.e., how confident the model is at each grid cell.

It can be observed from Figure 11 and 12 that the variance of the predicted Co or Ni concentrations is relatively low. This indicates the models —exponential model for Co and spherical model for Ni —are relatively more confident about the predictions.

### Comparison of predicted Co concentrations with variance

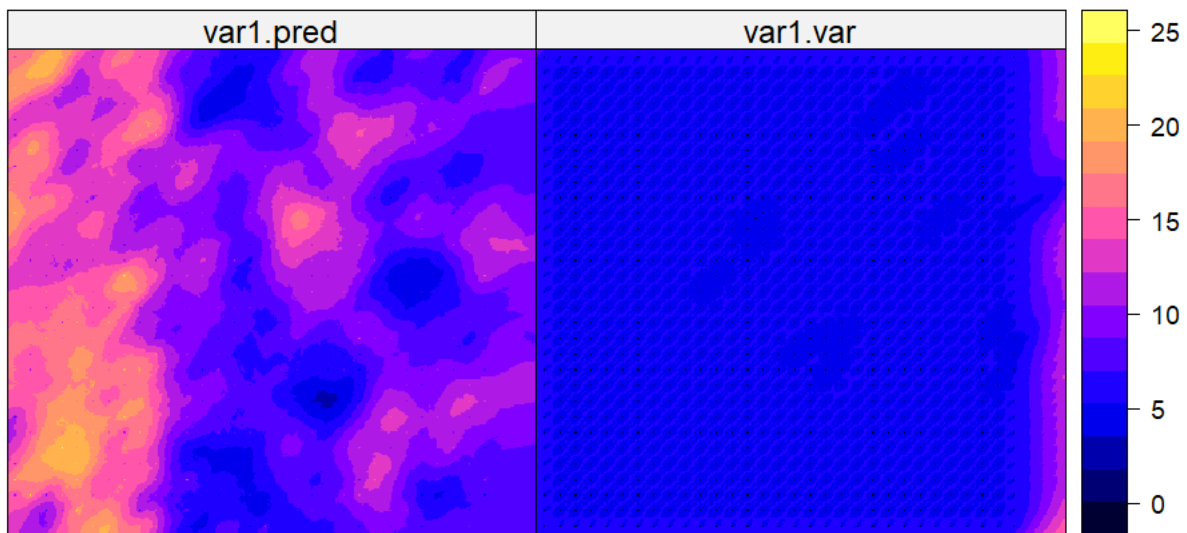


Figure 11: Predicted 'Co' concentrations with their variance across the grid using ordinary kriging.

### Comparison of predicted Ni concentrations with variance

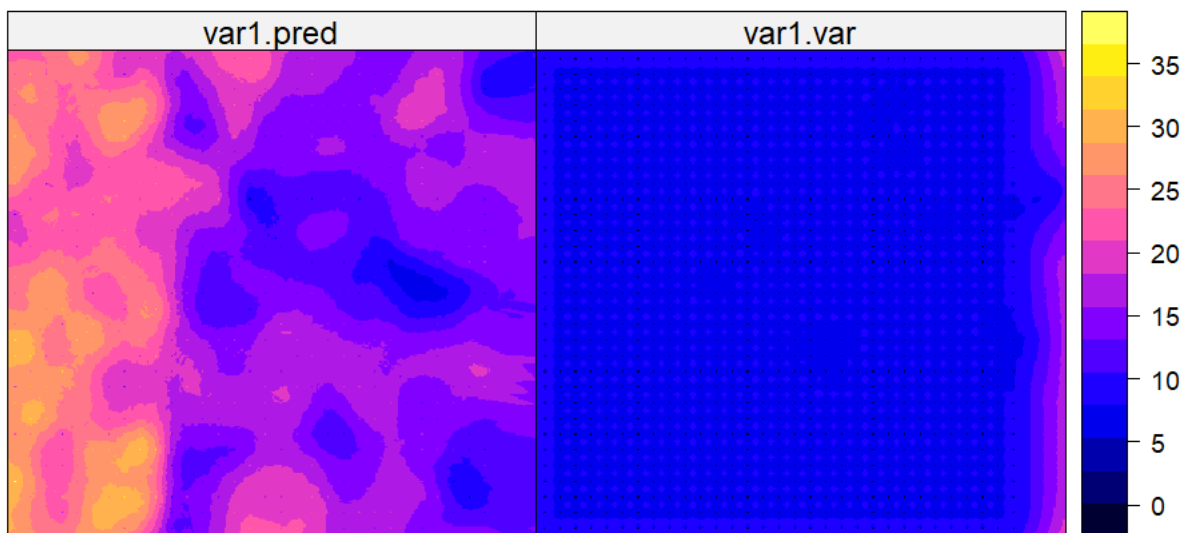


Figure 12: Predicted 'Ni' concentrations with their variance across the grid using ordinary kriging.

## 1.4. Cross Validation: Evaluation of Kriging analysis

To validate the predictions, a leave one out strategy is employed. During this leave one out strategy, concentration of a Co/Ni is predicted with trained variogram model after removing each sample from the data.

```
> summary(mcv_co)
Object of class SpatialPointsDataFrame
Coordinates:
  min max
x    0 3271
y    0 3000
Is projected: NA
proj4string : [NA]
Number of points: 994
Data attributes:
  var1.pred    var1.var    observed    residual    zscore    fold
Min.   : 3.791  Min.   :4.236  Min.   : 0.766  Min.   :-9.199412  Min.   :-3.927809  Min.   : 1.0
1st Qu.: 7.922  1st Qu.:5.486  1st Qu.: 7.554  1st Qu.: -1.477840  1st Qu.: -0.621461  1st Qu.:249.2
Median :10.010  Median :5.486  Median :10.236  Median : 0.052062  Median : 0.022228  Median :497.5
Mean   :10.655  Mean   :5.505  Mean   :10.655  Mean   :-0.000647  Mean   :-0.000253  Mean   :497.5
3rd Qu.:13.249  3rd Qu.:5.486  3rd Qu.:13.042  3rd Qu.: 1.448652  3rd Qu.: 0.618334  3rd Qu.:745.8
Max.   :20.524  Max.   :8.578  Max.   :24.368  Max.   : 8.571795  Max.   : 3.658954  Max.   :994.0
```

Figure 12: Summary of cross validation metrics for Co using exponential model

```
> sd_co <- sd(mcv_co$residual)
> sd_co
[1] 2.40918
```

Figure 13: Standard deviation of residuals for Co using exponential model

It is observed that the standard deviation of residuals is 2.409, which is reasonably small as its 10% of the total range 0.7566 to 24.368. Also, the mean of the residuals is almost 0. As a result, the exponential model used for estimation of Co concentrations can be relied upon and resemble the actual Co data.

Similarly, from Figure 14 and 15, we could infer that standard deviation of Ni residuals is 2.78, which is even smaller than Co as the range of observed values is from 2.73 to 36.55. Also, the mean of residuals is almost 0.



```
> summary(mcv_ni)
Object of class SpatialPointsDataFrame
Coordinates:
  min  max
x    0 3271
y    0 3000
Is projected: NA
proj4string : [NA]
Number of points: 994
Data attributes:
  vari1.pred      vari1.var      observed
Min.   : 7.535      Min.   : 7.426      Min.   : 2.731
1st Qu.:14.440      1st Qu.: 8.454      1st Qu.:13.978
Median :16.747      Median : 8.456      Median :17.022
Mean   :18.040      Mean   : 8.498      Mean   :18.038
3rd Qu.:22.277      3rd Qu.: 8.456      3rd Qu.:21.820
Max.   :29.644      Max.   :12.225      Max.   :36.554
  residual      zscore      fold
Min.   :-11.158883      Min.   : -3.709717      Min.   : 1.0
1st Qu.: -1.567512      1st Qu.: -0.538676      1st Qu.:249.2
Median : 0.009555      Median : 0.003286      Median :497.5
Mean   : -0.002721      Mean   : -0.000744      Mean   :497.5
3rd Qu.: 1.560976      3rd Qu.: 0.535242      3rd Qu.:745.8
Max.   : 10.773700      Max.   : 3.705054      Max.   :994.0
```

Figure 14: Cross validation results summary for Ni

```
> sd_ni<- sd(mcv_ni$residual)
> sd_ni
[1] 2.781768
```

Figure 15: Standard deviation of Ni using spherical variogram model

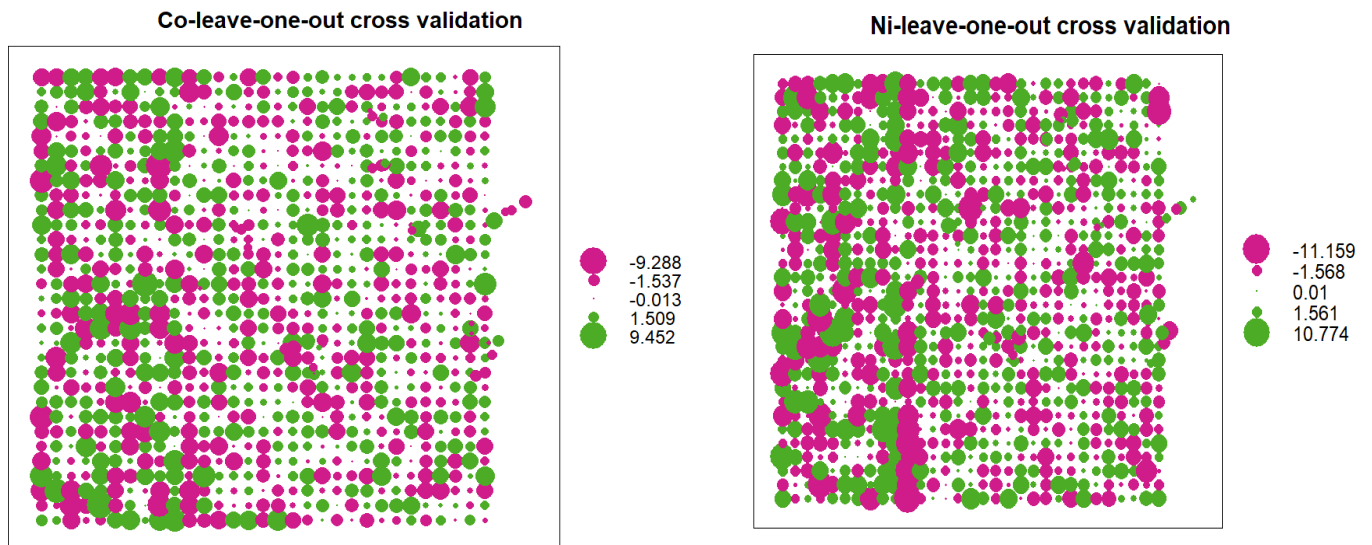


Figure 16: Bubble plot indicating the size of residuals for Co and Ni.

## 2. Variogram and analysis based on sub regions of high concentrations and low concentrations

### 2.1. Comparison of subregions kriging a with Overall-Area Results

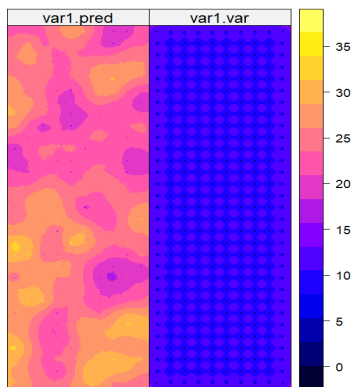
As identified in the exploratory data analysis Figure5, there is a high concentration of Co and Ni at  $x < 1000\text{m}$  and low concentration at  $x > 1000\text{m}$ . So, they are separated into 2 datasets. As before, kriging analysis is performed on both the datasets.

It can be observed from Table2 that, the standard deviations for kriging during cross validation for  $x < 1000\text{m}$  is higher than the standard deviations during cross validation for  $x > 1000\text{m}$ . This is due to the presence of high concentrations of Co and Ni on the left side( $x < 1000\text{m}$ ), which led to big residuals.

Analysis	Overall area		$x < 1000\text{m}$		$x > 1000\text{m}$	
	Co	Ni	Co	Ni	Co	Ni
Check for anisotropy	Present	Present	Mostly isotropic	Mostly isotropic	Mostly isotropic	Mostly isotropic
Variogram model	Exponential model	Spherical model	Exponential model	Spherical model	Exponential model	Spherical model
Variogram Parameters	Range:1250m Nugget:2 Sill:18	Range:1400m Nugget:2 Sill :30	Range:1250 Nugget:2 Sill :18	Range:1400 m Nugget:2 Sill :30	Range:1250 Nugget:2 Sill :18	Range:1400 m Nugget:2 Sill :30
Fit with the data	Fit not achieved at all angles	Fit not achieved at all angles	Good fit achieved	Good fit achieved	Good fit achieved	Good fit achieved
Kriging type	Ordinary kriging	Ordinary kriging	Ordinary kriging	Ordinary kriging	Ordinary kriging	Ordinary kriging
Standard deviation of kriging cross-validation	2.409	2.781	3.157	3.415	1.970	2.052

Table 2: Summary of kriging analysis results on comparison with  $x < 1000\text{m}$  and  $x > 1000\text{m}$  with overall area.

Comparison of predicted Ni concentrations with variance



Comparison of predicted Co concentrations with variance

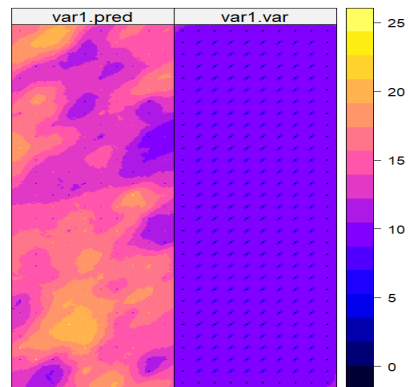
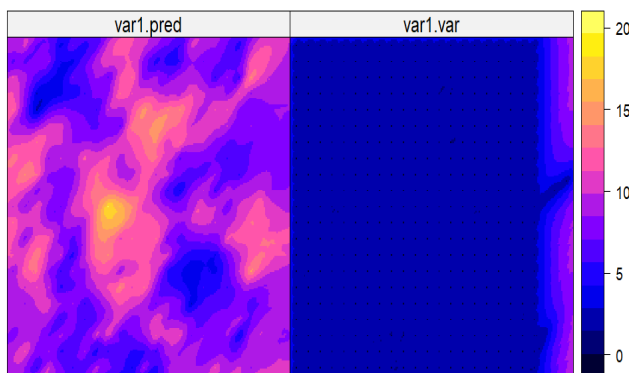


Figure 17: Kriging prediction of Co and Ni concentrations with its variance for  $x < 1000m$  data

Comparison of predicted Co concentrations with variance



Comparison of predicted Ni concentrations with variance

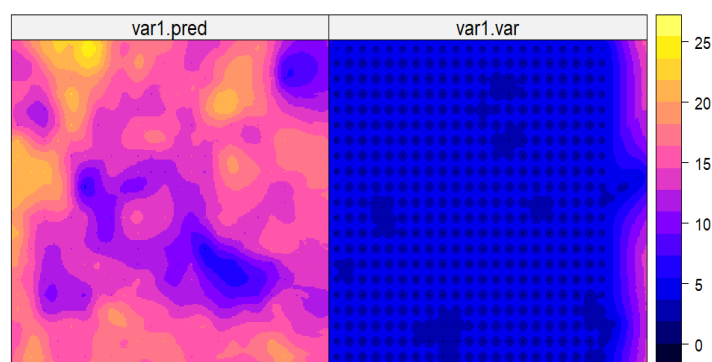


Figure 18: Comparison of Co and Ni predictions with its variance for  $x > 1000m$  data.

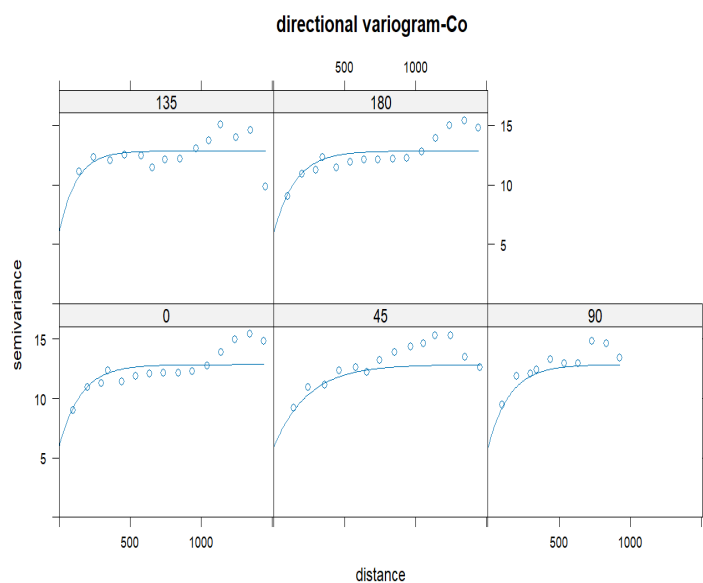


Figure 19: Directional variogram of Co and Ni concentrations for  $x < 1000$  data

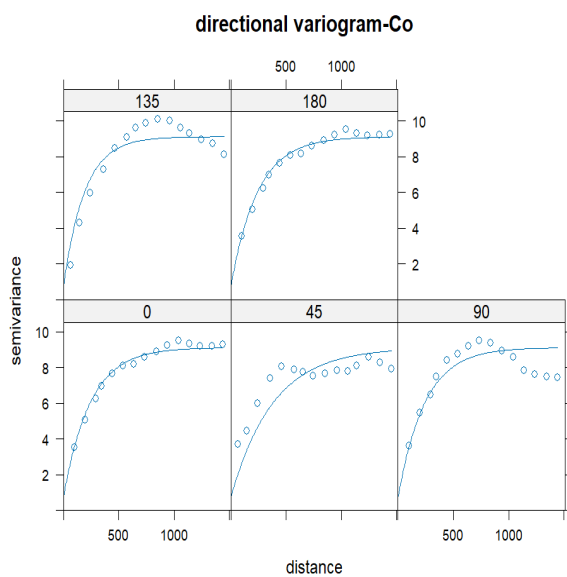
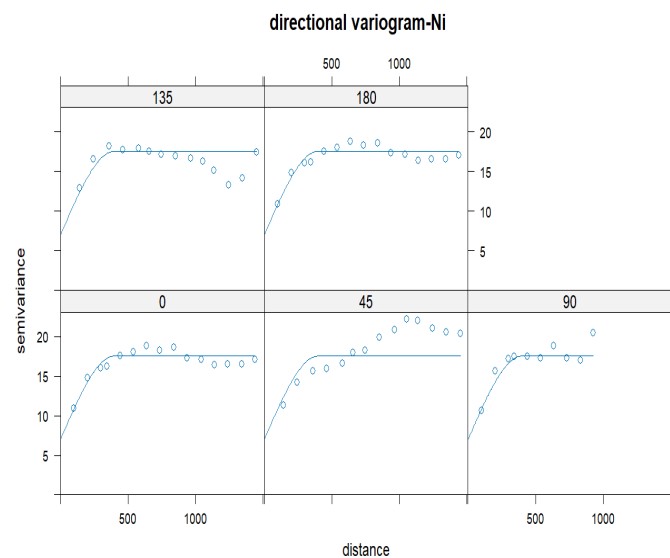


Figure 20: Directional variogram of Co and Ni concentrations for  $x > 1000m$  data

